

ScienceDirect



IFAC PapersOnLine 58-28 (2024) 306-311

Sensor-Fusion-based Optimal Multi-Disturbance Filtering in Atomic Force Microscope Imaging

Jiarong Chen* Qingze Zou**

* Department of Mechanical and Aerospace Engineering Rutgers, The State University of New Jersey New Brunswick, New Jersey 08901 Email: jiarong.chen@rutgers.edu ** Email: azzou@rutgers.edu

Abstract: This paper presents a data-driven filtering technique to optimally reduce/remove the distortions caused by multiple disturbances from unknown locations in atomic force microscope (AFM) image. AFM measurement is sensitive to external disturbances including acoustic signals and mechanical vibrations, as disturbance to the probe-sample interaction directly results in distortions in the sample images obtained. Although conventional passive noise cancellation has become the industry standard, limitation exists and residual noise still persists. The disturbance dynamics involved, are complicated, broadband, and not decaying with frequency increase. Even more challengingly, acoustic and mechanical vibration cancellation, is complicated by the co-existence of multiple noise/vibration sources and heterogeneous dynamic effects of these disturbances on AFM imaging. In this work, we propose a sensor-fusion-based technique to optimize the measurement of the overall disturbance signal, and minimize the disturbance-caused image distortions. The technique is illustrated by implementing it to filter calibration and silicon sample images under the effect of both acoustic noise and mechanical vibration. The experimental results are discussed to demonstrate that the image distortion was substantially further reduced by the proposed technique than using any individual signal.

Copyright © 2024 The Authors. This is an open access article under the CC BY-NC-ND license (https://creativecommons.org/licenses/by-nc-nd/4.0/)

Keywords: Active Noise Filtering, AFM Imaging, Sensor Fusion.

1. INTRODUCTION

In this paper, a data-driven sensor fusion technique is proposed to optimally reduce/remove the distortion caused by multiple disturbances from unknown locations in atomic force microscope (AFM) image in atomic force microscope (AFM) image. As one of the most important instruments in nanoscale science and technology exploration (Sundararajan and Bhushan (2002)), AFM is sensitive to external disturbances including acoustic noise and mechanical vibrations, as these disturbances interfere the probesample interaction directly result in the distortion in AFM images (Gołek et al. (2014)). Although passive noise apparatuses (Ito et al. (2015); Benmouna and Johannsmann (2002)) have been employed to combat acoustic disturbance, such a de facto industry standard faces limitations in both performance, usability and cost. Moreover, acoustic and mechanical vibration cancellation, is complicated by the co-existence of multiple noise/vibration source and heterogeneous dynamic effects of these disturbances on AFM imaging. Thus, this work aims to tackle these challenges through the development of a sensor-fusion-based technique to minimize the effects of multiple acoustic and mechanical vibration disturbances on AFM image.

Techniques need to be developed to eliminate AFM image distortions caused by multiple external disturbances from arbitrary locations unknown a priori. It is important to maintain the probe-sample interaction accurately

around the set point value in AFM applications (Eaton and West (2010)). Although significant progresses have been achieved to account for/avoid the probe vibration caused by the excitation of the dynamics and hysteresis behaviors of the nanopositioning system in AFM—through hardware improvement (e.g., using piezo actuator and/or cantilever of higher bandwidth) (Schitter et al. (2007)), and/or software enhancement of more advanced control techniques (Ren and Zou (2014a,b); Wu and Zou (2009)). External disturbances (causing probe vibration) have been mainly accounted for via passive vibration/noise isolation apparatus. These passive apparatus are costly and bulky, not implementable when AFM needs to be integrated with other instrument like optical microscope. Moreover, residual image distortion still persists, and the image quality obtained cannot meet the stringent requirements such as in cleanroom nanometrology in semi-conductor industry (Ducourtieux and Poyet (2011)). Few work has been reported on active control or post-filtering of acoustic noise for AFM, not to mention the general scenario of co-existing multiple heterogeneous disturbances (acoustic and mechanical vibrations). Recently, a data-driven active acoustic noise control technique has been proposed to reject acoustic disturbance during AFM imaging (Sicheng Yi (2018)). Although this technique has been effectively demonstrated through experiments, its performance can be sensitive to the location of the acoustic source, particularly when the location of the disturbance is unknown

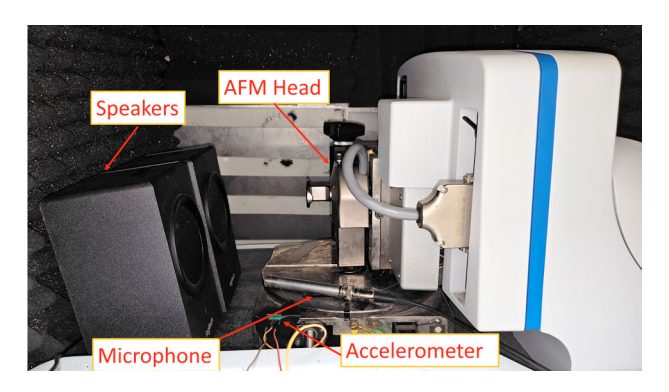


Fig. 1. An experimental setup for studying noise effect on AFM operation, where it is assumed that the location of the noise source (speakers) is unknown while the sensors (microphone and accelerometer) are placed at fixed and known locations.

and distant away from the sensor (i.e., microphone). This issue of arbitrary unknown acoustic disturbance has been addressed through a data-driven post-filtering technique where a library-based approach is developed to allocate the disturbance and account for the un-collocation of the disturbance and the sensor (Chen and Zou (2022a)). However, the construction of the acoustic propagation and acoustic dynamics libraries is time consuming and prone to the acoustic changes in AFM imaging. To tackle this challenge critical in practical implementations, an optimal filtering technique based on the Wiener filtering theory (Haykin (2013)) has been developed (Chen and Zou (2023)) to minimize the acoustic-caused image distortion caused by an arbitrary unknown disturbance, and has been extended to active online noise control in AFM imaging (Chen and Zou (2022b)). Although experimental implementation shows that the image quality can be recovered regardless the disturbance location, only the effect of a single acoustic disturbance is considered—issues related to signal to noise ratio and heterogeneous effects in multiple disturbance case have not yet been addressed. Thus, technique needs to be developed to combat multiple types of noise effect on AFM image.

The main contribution of this paper is the development of a data-driven sensor-fusion-based technique to minimized AFM image distortions caused by multiple heterogeneous disturbances. Specifically, the general problem of sensing optimization and disturbance rejection via post filtering using multiple sensor signals is considered. A coherence minimization based approach is proposed to optimally combine the multiple sensor signals measured, and then, minimize the overall image distortions. The filtering technique is purely data driven and does not require characterizing the acoustic/vibration dynamics a priori, providing robustness and ease of implementation in practical uses. The proposed fusion scheme is implemented on AFM image examples and the experimental results show that the image distortion are significantly reduced in complicated noisy environment.

2. SENSOR FUSION FOR MULTIPLE NOISE SOURCES

2.1 Problem Formulation

It is important in AFM applications to eliminate external disturbances including acoustic noise and mechanical vibrations. The basic principle of AFM measurement is to manipulate a nanometer-size cantilever-tip to interact with the sample and regulate the probe-sample interaction with nanoscale precision. Thus, external disturbances can induce extraneous perturbation to the probe-sample interaction, and thereby, loss of precision and quality in the AFM measurements (See Fig. 1). More specifically, during tapping-mode (TM) imaging of AFM, the cantilever tip is tapping on the sample surface at a frequency near the resonant frequency of the cantilever (driven by a dither piezo actuator) while scanning across the sampling surface (Hansma et al. (1994)). Provided that the tapping amplitude is kept closely around a pre-chosen constant level via feedback control so that the tip-sample interaction (i.e., the tip tapping) is well maintained, the sample topography image can be obtained from the (vertical) displacement of the cantilever. However, the mechanical structure of the AFM can be excited by environmental disturbances, resulting in unwanted cantilever vibration and thereby, image distortion.

The challenge arises as in general, multiple external disturbances such as acoustic noise and ground vibrations exist and couple together in affecting the imaging process. Moreover, The locations of the disturbances are usually unknown and might not be fixed, resulting in the so-called source-sensor non-collocation. This dynamic, source-sensor non-collocation imposes two challenges to the filtering of the image distortion caused by external disturbances: One, single sensor may not be adequate to capture multiple disturbance signals, and secondly, low SNR when the sensor is far away from the acoustic source. Hence, we propose a sensor-fusion based technique to optimally utilize multiple sensors to combat these two challenges.

Specifically, we aim to develop a post-imaging filtering technique to optimally reduce the AFM image distortion caused by multiple acoustic and ground vibration disturbances from different unknown locations. Without loss of generality, we assume that

Assumption 1: The locations of the disturbances are fixed but arbitrary and unknown.

Assumption 2: The disturbances $n_1[k], n_2[k], ..., n_m[k]$ are zero-mean, band-limited wide-sense stationary (WSS) random processes which are not correlated with each other, and the variation of their primary disturbance dynamics (PDD) is quasi static.

The PDD in Assumption 2 is the dynamics from the noise signal (as the input) to the AFM image signal (as the output response). Assumption 2 is reasonable as the variation of the PDD is mainly caused by the change of the noise source location, i.e., the noise propagation route and the AFM configuration (e.g., mounting of the cantilever),

both remain unchanged during an imaging process but otherwise can vary significantly in day-to-day operations.

In the presence of multiple disturbances, the measured AFM signals $z_m[k]$ becomes

$$z_m[k] = z_s[k] + z_{dst}[k], \text{ for } k = 0, \dots, N_I - 1,$$
 (1)

where $z_s[k]$ and $z_{dst}[k]$ are the z-axis piezo displacement corresponding to the sample topography and that due to the noises, and N_I is the total number of sampling data acquired in the given imaging process, respectively. As $z_m[k]$ is used to plot the sample topography image, in the following, $z_m[k]$, $z_s[k]$, and $z_{dst}[k]$ are called the measured image signal, the true sample image signal, and the combined image disturbance signal, respectively,

$$z_{dst}[k] = \sum_{i=1}^{m} z_i[k], \text{ for } k = 0, \dots, N_I - 1,$$
 (2)

with

$$z_i[k] = g_i[k] * n_i[k],$$
 (3)
for $i = 1, \dots, m$, and $k = 0, \dots, N_I - 1$,

where g[k] is the impulse response of the PDD of the respective noise (disturbance), m is the number of noises and "*" denotes convolution operations. Equivalently, the above combined disturbance can also be represented in the frequency domain as

$$Z_{dst}(j\omega_k) = \sum_{i=1}^{m} G_i(j\omega_k) N_i(j\omega_k) \text{ for } i = 1, \dots, m \quad (4)$$

Data-driven Optimal Filtering of Multi-Disturbance (DD-OFMD) AFM Image Distortion Let Assumptions 1-3 hold, the problem is to design a data-driven method to optimally combine the sensor signals, then design the optimal filter directly from the measured sensor signals (without a parameterized model), such that

 \mathbb{O} -1 The fused disturbance signal $n_t[k]$ is also a zero-mean WSS, and the SNR of the fused sensor signal is optimized that maximizes the effect of the disturbance on the measured AFM signal in the correlation sense, i.e.,

$$\max_{\hat{n}_t[k]} J_n = \mathbf{E} \{ \hat{n}_t[k-j] z_m[j] \}^2,$$
 (5)

 \mathbb{O} -2 The filter $\hat{g}_{dst}^*[k]$ is optimal such that the expectation of the disturbance-caused image distortion $e_I[k]$ between the true image and the filtered image is zero,

$$\mathbf{E}(e_I[k]) = \mathbf{E}\{z_T[k] - z_F[k]\} = 0 \tag{6}$$

and the variance of the distortion is minimized.

$$\min_{\hat{g}_{dst}^*[k]} J_z = \mathbf{E} \{ e_I[k] \}^2 \tag{7}$$

O-3 The fused signal and the filter are designed directly from the measured sensor signals (without a parameterized model).

We proceed by achieving the three objectives in order.

2.2 [O-1&2] Optimization of Fused Sensor Signal and Acoustic-Image Filter

In practice, the disturbances $N_i(j\omega_k)$ and the respective PDDs $G_i(j\omega_k)$ are unknown, and multiple sensors can be deployed. Therefore, we propose to fuse the RMS-normalized measured signals from multiple sensors to replace the unknown disturbances and construct a PDD $G_{dst}(j\omega_k)$ to represent the effect of the combined PDDs, i.e. we presume that

$$Z_{dst}(j\omega_k) = G_{dst}(j\omega_k)N_t(j\omega_k)$$

$$= G_{dst}(j\omega_k)\sum_{i=1}^{l} \alpha_i(j\omega_k)\hat{N}_i(j\omega_k)$$
(8)

where $\alpha_i(j\omega_k) \in (0,1)$ are the frequency-dependent weight coefficients, l is the number of sensors deployed and $\hat{N}_i(j\omega_k)$ is the discrete Fourier transform of the normalized measured signal $\hat{n}_i[k]$, i.e.,

$$\hat{n}_i[k] = \frac{n_{mi}[k]}{\sqrt{\frac{\sum_{j=1}^{N_i} n_{mi}[k]^2}{N_i}}} \text{ for } i = 1, \dots, l$$
 (9)

with $n_{mi}[k]$ the measured signal from the i^{th} sensor. To ensure the solution of weight α_i is unique, the weight coefficients are normalized as follows

$$\sum_{i=1}^{l} \alpha_i(j\omega_k) = 1 \tag{10}$$

In order to search the optimal set of weight coefficients $\alpha_i^*(j\omega_k)$, we propose to exploit the coherence, representation of the correlation in frequency domain (Welch (1967)), between the fused noise signal $N_t(j\omega_k)$ and the measured image signal $Z_m(j\omega_k)$

$$C_{nz}(j\omega_k) = \frac{\mathbf{E}^2[N_t^*(j\omega_k)Z_m(j\omega_k)]}{\mathbf{E}[N_t^2(j\omega_k)]\mathbf{E}[Z_m^2(j\omega_k)]}$$
(11)

such that

$$\min \mathcal{J}_c = \sum_{k=1}^{N_F} (1 - C_{nz}(j\omega_k))$$
 (12)

because the coherence represents the strength of relationship between the fused signal and the measured image signal. Hence, the α_i would optimize the SNR of disturbances measured by sensors.

We define the error $E(j\omega_k)$ as

$$E(j\omega_k) \triangleq Z_m(j\omega_k) - G_{dst}(j\omega_k)N_t(j\omega_k)$$
 (13)

By assumption 2

$$C_{nz}(j\omega_k) = \frac{[G_{dst}(j\omega_k)N_t(j\omega_k)]^2}{[G_{dst}(j\omega_k)N_t(j\omega_k)]^2 + E^2(j\omega_k)}$$
(14)

the maximal of $C_{nz}(j\omega_k)$ is achieved when $E(j\omega_k) = Z_s(j\omega_k)$ as $Z_s(j\omega_k)$ is not correlated to any disturbance

 $N(j\omega_k)$, \mathbb{S}_{ω} is the set of the sampled discretized frequencies,

$$\mathbb{S}_{\omega} = \left\{ \frac{k\omega_s}{N_I} \middle| k = 0, 1, \cdots, N_I - 1, \text{ and } \omega_s = 2\pi f_s \right\}$$
 (15)

 N_F denotes the total number of effective frequency components in the noise source n[k], i.e., ω_{N_F} is the lowest frequency at which the magnitude of $\hat{N}(j\omega_k)$ becomes negligible, e.g., $|\hat{N}(j\omega_k)| \leq \epsilon_n$ for all $\omega_k \geq N_F$ and chosen threshold ϵ_n .

Similarly, the optimal acoustic-image filter $g_{dst}[k]$ to minimize the error between the true image and the filtered image can be designed by optimizing the estimated true image $z_f[k]$ to minimize the power of correlation between the fused noise $n_t[k]$ and the filtered image $z_f[k]$ —It can be shown that minimizing the cost function J_z in Eq. (7) is equivalent to minimizing the following correlation \hat{J}_z :

$$\min \hat{J}_z = \mathbf{E}\{\hat{n}[k-j]z_f[j]\}^2 \tag{16}$$

where

$$z_f[k] = z_m[k] - g_{dst}[k] * n_t[k]$$
(17)

2.3 [O-3] Data-Driven Design Method

Next we present a data-driven approach to construct and implement the above optimal filter via coherence minimization. In practice, the optimal sensor fusion coefficients $\alpha_i^*(j\omega_k)$ s in Eq. (8) are obtained through the gradient descent search method, i.e., for any given $\omega_k \in \mathbb{S}_{\omega}$

$$\alpha_{i,j}(j\omega_k) = \alpha_{i,j-1}(j\omega_k) + \lambda \frac{\partial \mathcal{J}_c}{\partial \hat{N}_{j-1}(j\omega_k)}$$

$$= \alpha_{i,j-1}(j\omega_k) + \lambda \frac{\partial \mathcal{J}_c}{\partial \alpha_{i,j-1}(j\omega_k)} \frac{1}{N_i(j\omega_k)}$$
(18)

for $i \geq 1$, where initially $\alpha_{i,0}$ is chosen as $\frac{1}{l}$, $\lambda \in (0, 1)$ is a pre-chosen constant to ensure the increase of the coherence. The coefficient obtained after each iteration is normalized before the next iteration:

$$\hat{\alpha}_{i,j}(j\omega_k) = \frac{\alpha_{i,j}(j\omega_k)}{\sum_{i=1}^{l} \alpha_{i,j}(j\omega_k)}$$
(19)

Then, the optimal acoustic-image filter $g_{dst}[k]$ to minimize the error between the true image and the filtered image can be designed through the Wiener-filter-based modulator optimization approach. Specifically, the minimization of Eq. (16) yields a Wiener Filter as a solution

$$\hat{\mathbf{g}}_{dst}^* = \mathbf{R_n}^{-1} \mathbf{p_{nz}} \tag{20}$$

where $\mathbf{R_n}$ is the auto-correlation matrix of the fused noise, $\mathbf{n_t}$.

$$\mathbf{R_{n}} = \mathbf{E}\{\mathbf{n_{t}}\mathbf{n_{t}^{T}}\}$$

$$= \begin{bmatrix} R_{n}[0] & R_{n}[1] & \dots & R_{n}[N_{I}-1] \\ R_{n}[1] & R_{n}[0] & \dots & R_{n}[N_{I}-2] \\ \vdots & \vdots & \ddots & \vdots \\ R_{n}[N_{I}-1] & R_{n}[N_{I}-2] & \dots & R_{n}[0] \end{bmatrix}$$
(21)

and $\mathbf{p_{nz}} = \mathbf{E}\{\mathbf{n_t}\mathbf{z_m^T}\}$ is the cross-correlation between the fused noise $n_t^*[k]$ and the measured sample image signal

 $z_m[k]$, respectively. Then $\hat{\mathbf{g}}_{dst}^*$ is further enhanced by a coherence minimization technique. Readers can refer to ... for more details.

3. EXPERIMENT IMPLEMENTATION

The proposed approach was demonstrated through an AFM imaging experiment. The AFM imaging experiment was performed on a commercial AFM system (Dimension Icon, Bruker Nano Inc.), where the acoustic noise was induced by a speaker placed on the sample stage, and measured via a precision array microphone (BK 4958, Bruel Kjaer Inc.) and an acceleromter chip (ADXL203,Analog Devices), as shown in Fig. 1. The acoustic noise sensor signal was first pre-filtered and amplified using a homemade Op-Amp circuit, while the seismic vibration was measured directly. Both of them were measured via a data acquisition system (NI RIO, USB-7856R, National Instrument Inc.). All the filtering algorithms were designed and implemented in MATLAB (Mathworks Inc.).

First, the acoustic-noise-effected AFM images were acquired under the noise effects from the speaker. A calibration sample (STR-1800R) and a silicon sample were imaged at a scan rate of 5 Hz under contact mode when a band-limited (20-1kHz) white noise with zero-mean and constant variance of 100 dB was boardcasted to the room through the speaker, while the microphone and accelerometer were placed at a known and fixed location.

Then, to improve the SNR of total noise $n_t(k)$, the two measured signals were further fused and optimized by the modulator-based sensor fusion method (described in Sec. 2). The filtered images were obtained by using the optimized total noise and the optimized filters obtain by coherence minimization approach to obtain the filtered image. For comparison, the images were also filtered directly by using the acoustic noise only and seismic vibration only.

Results and Discussions

The experimental results are shown in Figs. (2)-(6). The PDDs from the accelerometer, microphone signal and the fused sensor signal to the corresponding estimated noise distortion were quantified by measuring its error with that from the corresponding sensor signal to the "real" distortion (difference from the raw image and the reference image) in Fig. 3. The raw noise-effect images of the calibration sample and the silicon sample are compared to those filtered by using the accelerometer only, the microphone only and the fused signal in Fig. 2, respectively. Then, the line comparison of the filtering results are shown Fig. 5. The quantification of 2-norm errors are shown in Fig 6.

The imaging results demonstrated that the distortion caused by acoustic noise from an arbitrary unknown location can be substantially further reduced by using the proposed approach comparing to using any single sensor. First, the PDD was captured more accurately when using the fused signal, specifically at the frequency range near 200 Hz and 500 - 700 Hz. The error of PDD was significantly further reduced (see Fig. 3). Such an improvement in the PDD estimation resulted in the better elimination of the acoustic-caused image distortion while maintaining

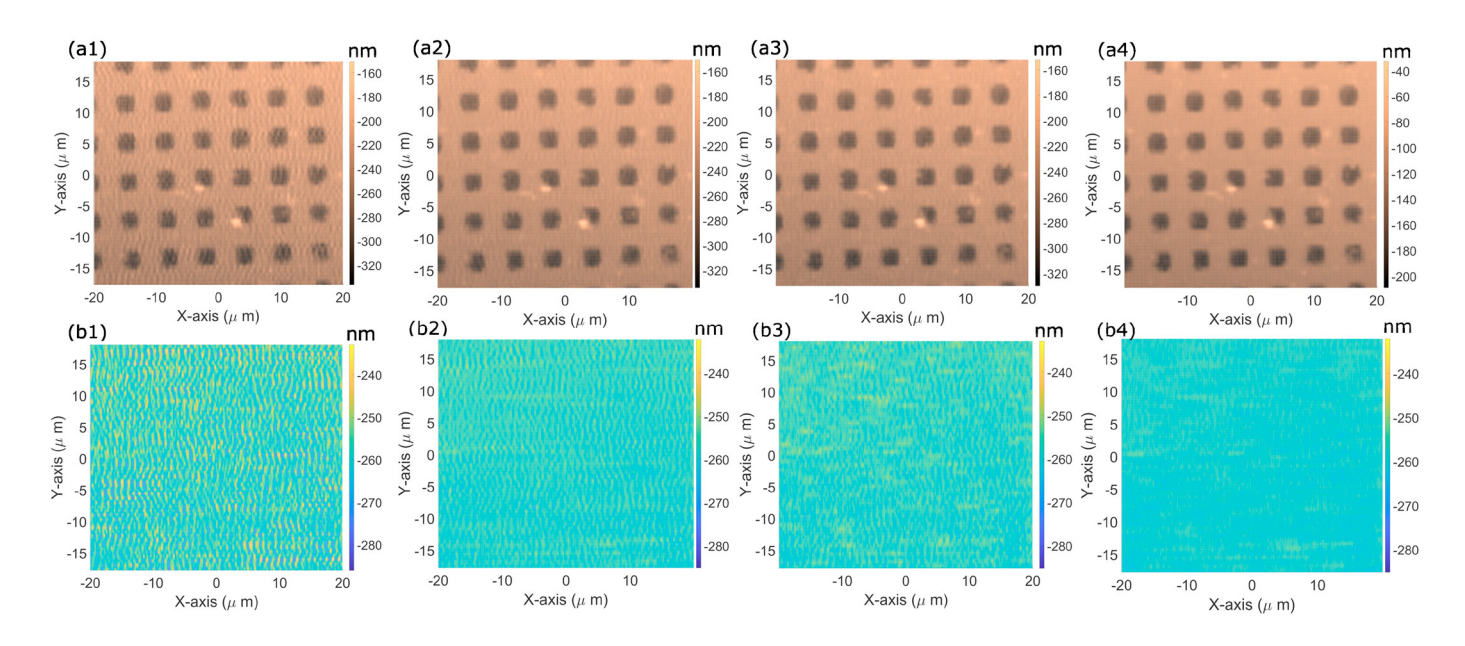


Fig. 2. Comparison of the original raw images obtained at a scan rate of 5 Hz (a1,b1) under the induced acoustic noise, and those filtered by (a2,b2) using the accelerometer only, and (a3,b3) using the microphone only and (a4,b4) using the proposed fused signal for (top row) the calibration sample and (second row) the silicon sample, respectively.

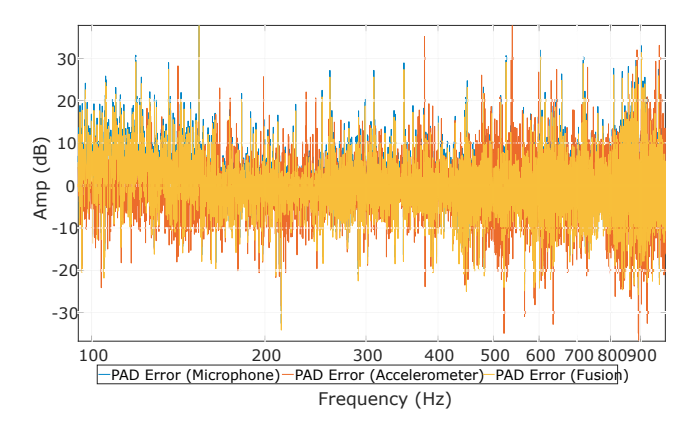
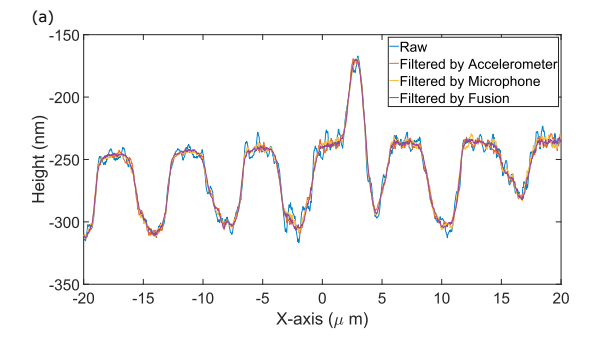


Fig. 3. The error (magnitude part) of the estimated dynamics using accelerometer, microphone and that of the sensor fusion method compared to the actual PDD, respectively.

the sample topography features. As shown in Fig. 2 (a1-a4), by using the proposed, the acoustic-caused image distortion was better removed and much closer to reference image quality (see Fig. 2 (a4)), whereas when using only one sensor, the edge of the pitches and the flat surface part were more smeared in the filtered image (see Fig. 2 (a2-3)). Such comparison was more obviously shown on silicon sample (see Fig. 2 (b1-b4)). To be specific, the relative 2-norm error was reduced by 72%-82% by using individual sensor, and then further by another 10%-15% by using the proposed sensor fusion technique. Therefore, the experimental results demonstrated the efficacy of the proposed approach.

4. CONCLUSION

A data-driven sensor fusion technique was developed to eliminate AFM image distortion caused by multiple or



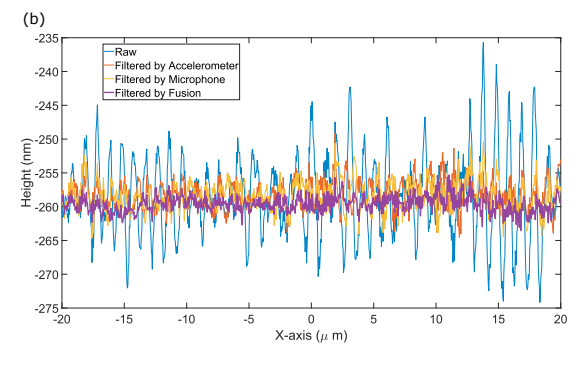


Fig. 4. The line comparisons of filtered signals using accelerometer only, microphone only, and that of the sensor fusion method compared to the measured image signal of (a) calibration sample and (b) silicon sample, respectively.

different type of noises using sensor array. The coherence relationship between noises and raw image is exploited to combine the signals and improve the SNR of the fused sensor signal. It is shown that by introducing a modulator weight to each noise signal, the error in the estimated acoustic dynamics and the low SNR of the measured acoustic noise can be eliminated by optimizing the modulator

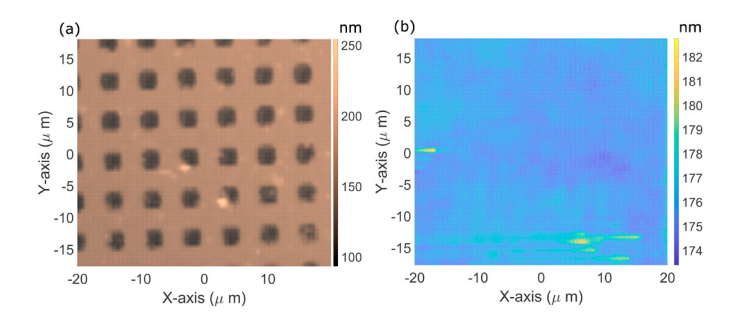


Fig. 5. The reference image of (a) calibration sample and (b) silicon sample acquired in quiet environment, respectively.

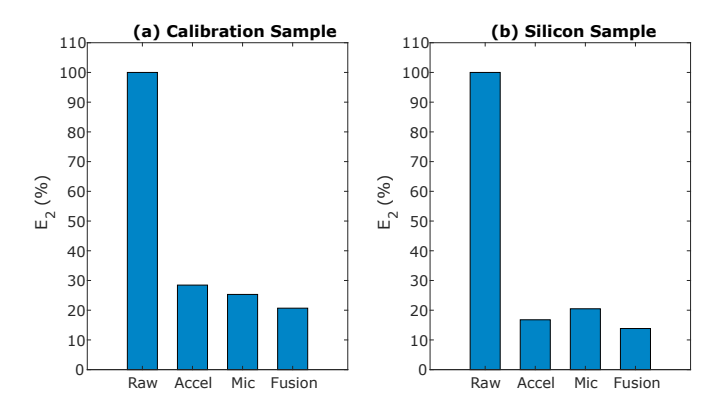


Fig. 6. Comparison of the normalized image error (with respect to the raw image error) for (a) the calibration sample and (b) the silicon sample in 2-norm, respectively.

via a gradient-based coherence minimization approach. The efficacy of the proposed approach was demonstrated by filtering experimentally measured AFM images. The results showed that the image distortion was substantially further reduced by the proposed technique than using any individual signal.

ACKNOWLEDGEMENTS

The financial support of NSF grants CMMI-1851907, IIBR-1952823, PFI-2234449, and NSF-PHY 2412551 are gratefully acknowledged.

REFERENCES

Benmouna, F. and Johannsmann, D. (2002). Hydrodynamic interaction of afm cantilevers with solid walls: An investigation based on afm noise analysis. The European Physical Journal E, 9(1), 435-441.

Chen, J. and Zou, Q. (2022a). Data-driven dynamics-based optimal filtering of acoustic noise at arbitrary location in atomic force microscope imaging. *Ultramicroscopy*, 242, 113614.

Chen, J. and Zou, Q. (2022b). Noise rejection mode imaging of atomic force microscope. IFAC-PapersOnLine, 55(37), 113–118.

Chen, J. and Zou, Q. (2023). Data-driven robust acoustic noise filtering for atomic force microscope image. In 2023 IEEE/ASME International Conference on Advanced Intelligent Mechatronics (AIM), 99–104. IEEE.

Ducourtieux, S. and Poyet, B. (2011). Development of a metrological atomic force microscope with minimized abbe error and differential interferometer-based real-time position control. *Measurement Science and Technology*, 22(9), 094010. doi:10.1088/0957-0233/22/9/094010.

Eaton, P. and West, P. (2010). Atomic force microscopy. Oxford university press.

Golek, F., Mazur, P., Ryszka, Z., and Zuber, S. (2014). Afm image artifacts. Applied surface science, 304, 11–19

Hansma, P., Cleveland, J., Radmacher, M., Walters, D.,
Hillner, P., Bezanilla, M., Fritz, M., Vie, D., Hansma,
H., Prater, C., et al. (1994). Tapping mode atomic force
microscopy in liquids. Applied Physics Letters, 64(13),
1738–1740.

Haykin, S.S. (2013). Adaptive filter theory[M]. Pearson Education India.

Ito, S., Neyer, D., Pirker, S., Steininger, J., and Schitter, G. (2015). Atomic force microscopy using voice coil actuators for vibration isolation. In 2015 IEEE International Conference on Advanced Intelligent Mechatronics (AIM), 470–475. IEEE.

Keyvani, A., van der Veen, G., Tamer, M.S., Sadeghian, H., Goosen, H., and van Keulen, F. (2020). Realtime estimation of the tip-sample interactions in tapping mode atomic force microscopy with a regularized kalman filter. *IEEE Transactions on Nanotechnology*, 19, 274– 283. doi:10.1109/TNANO.2020.2974177.

Ren, J. and Zou, Q. (2014a). High-speed adaptive contact-mode atomic force microscopy imaging with near-minimum-force. Review of Scientific Instruments, 85(7), 073706.

Ren, J. and Zou, Q. (2014b). High-speed adaptive contact-mode atomic force microscopy imaging with near-minimum-force. Review of Scientific Instruments, 85(7), 073706.

Ruppert, M.G., Karvinen, K.S., Wiggins, S.L., and Moheimani, S.R. (2015). A kalman filter for amplitude estimation in high-speed dynamic mode atomic force microscopy. *IEEE Transactions on Control Systems Technology*, 24(1), 276–284.

Schitter, G., Astrom, K.J., DeMartini, B.E., Thurner, P.J., Turner, K.L., and Hansma, P.K. (2007). Design and modeling of a high-speed afm-scanner. *IEEE Transactions on Control Systems Technology*, 15(5), 906–915.

Sicheng Yi, Tianwei Li, Q.Z. (2018). Active control of acoustics-caused nano-vibration in atomic force microscope imaging. *Ultramicroscopy*, 195, 101–110.

Sundararajan, S. and Bhushan, B. (2002). Development of afm-based techniques to measure mechanical properties of nanoscale structures. Sensors and actuators A: Physical, 101(3), 338–351.

Welch, P. (1967). The use of fast fourier transform for the estimation of power spectra: A method based on time averaging over short, modified periodograms. *IEEE Transactions on Audio and Electroacoustics*, 15(2), 70– 73. doi:10.1109/TAU.1967.1161901.

Wu, Y. and Zou, Q. (2009). An Iterative-Based Feedforward-Feedback Control Approach to High-Speed Atomic Force Microscope Imaging. *Journal of Dynamic* Systems, Measurement, and Control, 131(6).